

MODELING FLOOD INUNDATION DUE TO DAM AND LEVEE BREACH

Xinya Ying¹ and Sam S. Y. Wang²

ABSTRACT

The CCHE2D-FLOOD model has been developed to simulate flood inundation due to dam and levee breach. The model solves the conservative form of the two-dimensional shallow water equations using the finite volume method. The intercell flux is computed by upwind method and the water-level-gradient is evaluated by weighted average of both upwind and downwind gradient. The model adopts the raster grid so that GIS DEM can be directly imported into the model. The developed model is tested with a partial dam-break problem and two real-life cases of dam-break flows. It is shown that the CCHE2D-FLOOD model can correctly account for complex real-life dam-break flows which may include discontinuities, mixed flow regimes, and irregular geometry and giving a satisfactory prediction of the major characteristics such as water depth, flood extent, and flood wave arrival time. It is also demonstrated that the model is robust, computationally efficient and easy to use.

1. INTRODUCTION

Flood inundation due to dam and levee breach often cause serious loss of life and property. The numerical model can be used to predict flood wave propagation and provide the information about the flood extent, flood wave arrival time and water depth etc. Therefore, it is a useful tool for establishing flood control and dam operating strategies as well as developing evacuation plans and warning systems for the areas having potential flood risk.

In the present study, a two-dimensional numerical model is developed based on a finite volume method. The intercell flux is computed by upwind method and water-level-gradient is evaluated by weighted average of both upwind and downwind gradient. Therefore, the conservation of mass and momentum are guaranteed and the scheme is easy to implement. The proposed scheme is extensively tested with various examples with analytic solutions or measured data from physical models and field observations. This paper presents three selected test examples, including a partial dam-break problem and two real-life dam-break cases with complicated geometry. The numerical results are compared with experimental data.

¹ Research Scientist, National Center for Computational Hydroscience & Engineering, The University of Mississippi, 102 Carrier Hall, University, MS 38677, USA. Phone: 1-662-915-6564 Fax: 1-662-915-7796 Email: ying@ncche.olemiss.edu

² F.A.P. Barnard Distinguished Professor & Director, National Center for Computational Hydroscience & Engineering, The University of Mississippi, Carrier Hall Room 102, P.O. Box 1848, University, MS 38677-1848, USA. Phone: 1-662-915-6562 Fax: 1-662-915-7796 Email: wang@ncche.olemiss.edu

2. MODEL FORMULATION

2.1 Governing Equations

The conservative form of the two-dimensional shallow water equations is written as

$$\frac{\partial \mathbf{U}}{\partial t} + \frac{\partial \mathbf{F}}{\partial x} + \frac{\partial \mathbf{G}}{\partial y} = \mathbf{S} \quad (1)$$

where \mathbf{U} , $\mathbf{F}(\mathbf{U})$, $\mathbf{G}(\mathbf{U})$ and $\mathbf{S}(\mathbf{U})$ are respectively the vectors of conserved variables, fluxes in the x and y directions, and sources, defined as follows.

$$\mathbf{U} = \begin{bmatrix} h \\ hu \\ hv \end{bmatrix} \quad \mathbf{F} = \begin{bmatrix} hu \\ hu^2 \\ huv \end{bmatrix} \quad \mathbf{G} = \begin{bmatrix} hv \\ huv \\ hv^2 \end{bmatrix} \quad \mathbf{S} = \begin{bmatrix} 0 \\ -gh \frac{\partial Z}{\partial x} - g \frac{u\sqrt{u^2+v^2}}{C^2} \\ -gh \frac{\partial Z}{\partial y} - g \frac{v\sqrt{u^2+v^2}}{C^2} \end{bmatrix} \quad (2)$$

where h = water depth; u = velocity component in the x direction; v = velocity component in the y direction; g = gravitational acceleration; Z = water level; C = Chezy's channel resistance coefficient.

2.2 Numerical Method

The proposed upwind conservative scheme is based on the finite volume method. The model employs a rectangular raster grid, as shown in Figure 1, in order to directly use GIS raster topographic data. The conserved variables are defined at the cell centers and represent the average value over each cell, while the fluxes are calculated at the interfaces between cells.

Integrating (1) over the cell ij with area of $\Delta x_i \Delta y_j$ and applying Green's theorem yields

$$\mathbf{U}_{i,j}^{n+1} = \mathbf{U}_{i,j}^n - \frac{\Delta t}{\Delta x_i} (\mathbf{F}_{i+1/2,j} - \mathbf{F}_{i-1/2,j}) - \frac{\Delta t}{\Delta y_j} (\mathbf{G}_{i,j+1/2} - \mathbf{G}_{i,j-1/2}) + \Delta t \mathbf{S}_{i,j} \quad (3)$$

where $\mathbf{F}_{i+1/2,j}$, $\mathbf{F}_{i-1/2,j}$, $\mathbf{G}_{i,j+1/2}$, and $\mathbf{G}_{i,j-1/2}$ are the fluxes at the interfaces (see Figure 1). There are many approaches to evaluate the intercell fluxes that will construct various conservative numerical methods. The present model employs the one-side upwind method to evaluate the intercell fluxes. In order to avoid numerical oscillation and unphysical solutions, the water surface gradient in the source terms S_{ij} is computed by weighted average of downwind and upwind water surface gradients

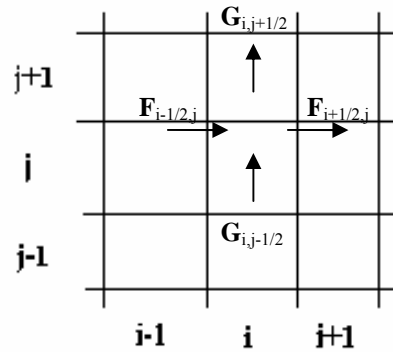


Figure 1 Definition sketch of a cell centered grid

using the local Courant number as a biased function. The friction term is explicitly computed based on the approximation that the variables are piecewise constant.

The proposed scheme is a two-step scheme. In first step, the continuity equation is solved and the water depth at $n+1$ time step is obtained. Then, in second step, the momentum equation is solved and the unit discharge at $n+1$ time step is calculated. Both the continuity and momentum equations are solved explicitly. Like most explicit schemes, this scheme is subject to the Courant-Friedrich-Lewy stability condition. The details about the numerical scheme and dry bed treatment are described in the references (Ying et al. 2003 and Ying et al 2004).

3. NUMERICAL TESTS

To validate the numerical model, three test examples are selected. Example 1 is a partial dam-break problem, which tests the performance of the model when the solution has discontinuities as well as the transition from subcritical flow to supercritical flow. Examples 2 and 3 are selected to test the model's capability to deal with real-life problems with complicated topography.

3.1 Partial Dam-Break Test Case

The model is validated against the experimental data of flood wave propagation due to a partial dam-break (Fraccarollo and Toro 1995). The reservoir is 1 m long and 2 m wide and the floodplain is 3 m long and 2 m wide (see Fig. 2). The breach is 0.4 m wide and located at the middle of the dam. The three boundaries of the floodplain are all open. In the selected case, the initial water depth in the reservoir is 0.6 m. The floodplain is initially dry. The bottom of the reservoir and floodplain is horizontal. The locations of five stations for measuring stage hydrographs are shown in Fig. 2 and their coordinates are listed in Table 1.

Table 1. Locations of stage gauges

Stations	-5A	C	4	0	8A
x (m)	0.18	0.48	1.00	1.00	1.722
y (m)	1.00	0.40	1.16	1.00	1.00

The computational domain is discretized into rectangular cells with $\Delta x = 0.04$ m, $\Delta y = 0.08$ m. Fig. 3 presents the measured results and the computed results by the current model and TVD-MacCormack method (Tseng and Chu 2000). The overall agreement between the measured and the computed results is reasonable. After the sudden opening of the gate, a surge is formed and propagates over the floodplain. Simultaneously, a strong depression wave occurs in the reservoir and causes the water surface near the gate to descend drastically. Because of the effects of boundary reflection, water surface in the reservoir oscillates significantly in the initial stage. All these details are well reproduced by the numerical model.

3.2 Malpasset Dam-Break Flood Simulation

The Malpasset dam was located in a narrow gorge of the Reyran river valley in France. It was a 66.5 m high arch dam with a crest length of 223 m and the maximum reservoir capacity of 55×10^6 m³. In the immediate downstream of the dam, the Reyran river valley is very narrow and has two consecutive sharp bends. Then the valley widens as it goes downstream and eventually reaches the

flat plain. The dam failed in 1959 following an exceptionally heavy rain. After the dam failure, a field survey was performed to obtain the maximum water levels along the river valley. In addition,

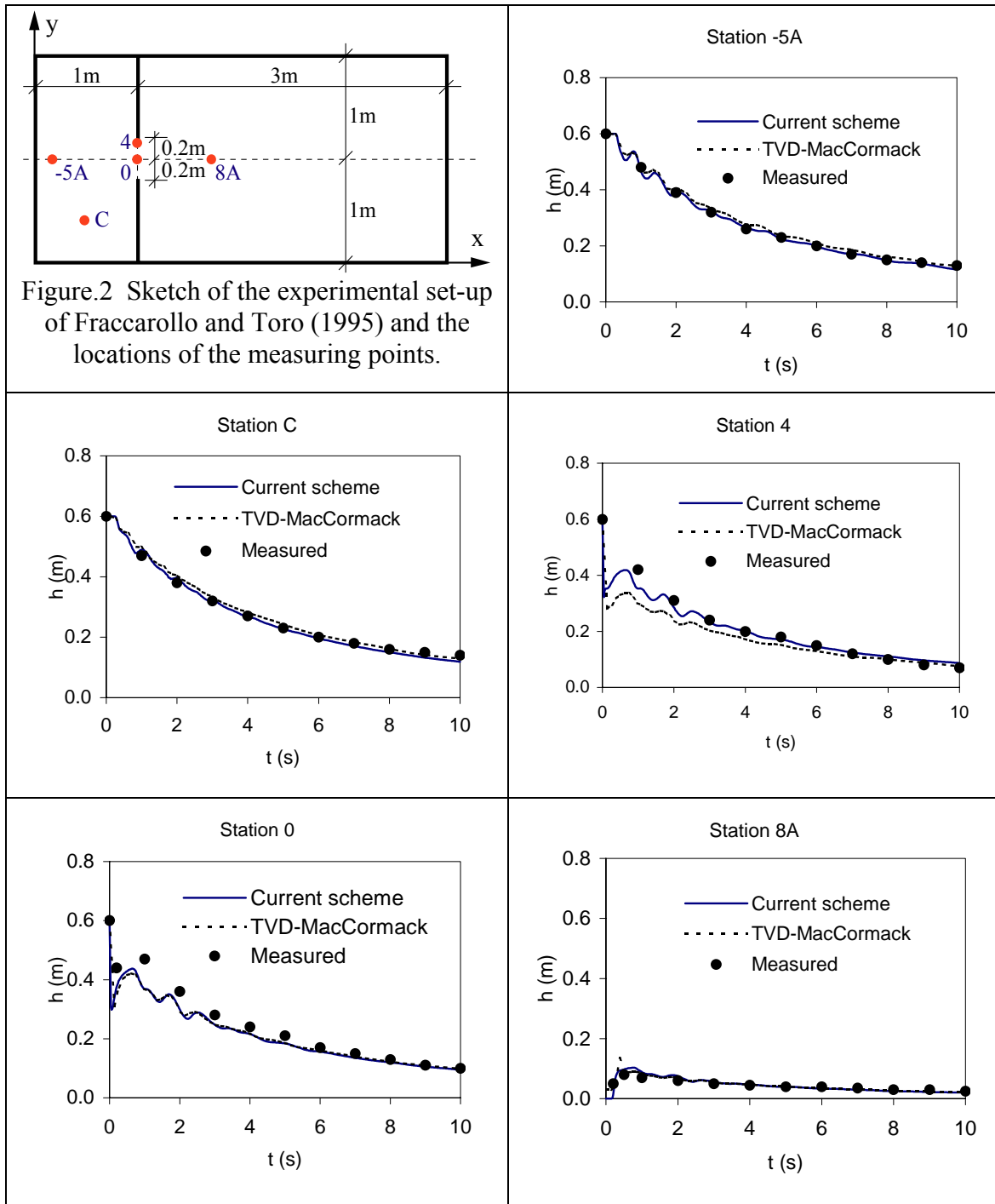


Figure. 3 Results of the partial dam-break test case.

a physical model with a scale of 1/400 was built to study the dam-break flow in 1964. The maximum water level and flood wave arrival time at 9 points along the river valley were measured.

A view of the river valley and locations of measuring points are shown in Figure 4. Because of its complex topography and availability of measured data, the Malpasset dam-break case was selected as a benchmark test example for dam-break models in the CADAM projects (Goutal 1999).

More detailed descriptions about the Malpasset dam-break test case can be found in literature (e.g. Goutal 1999 and Valiani et al. 2002).

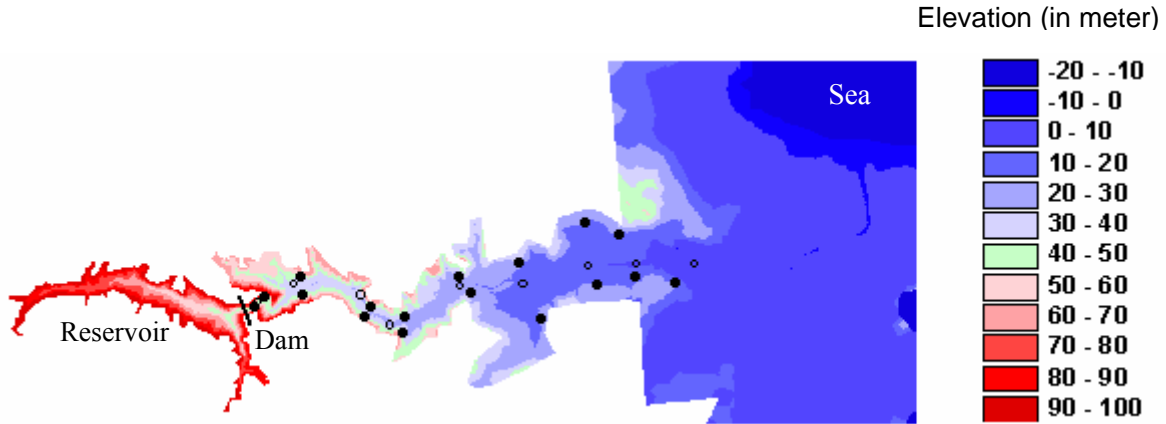
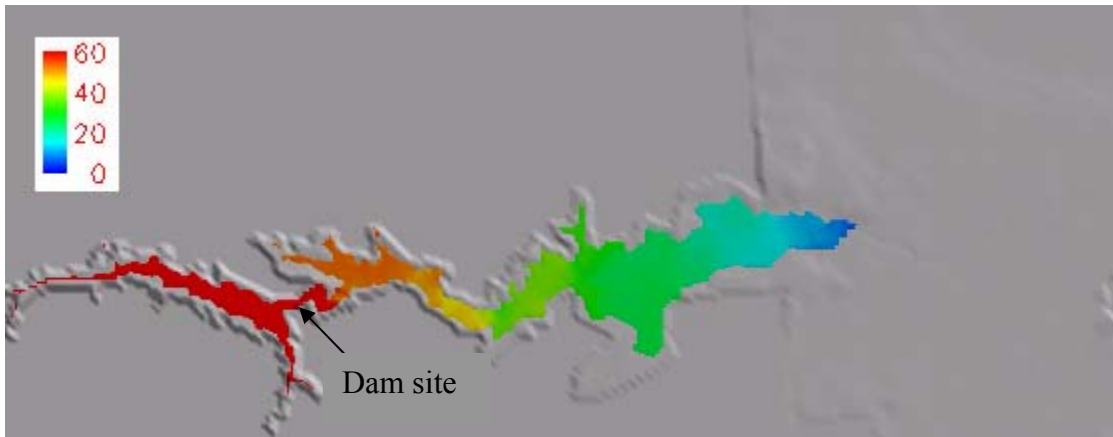


Figure 4. Topography and locations of measuring points for the Malpasset dam-break case (● field survey, ○ physical model)

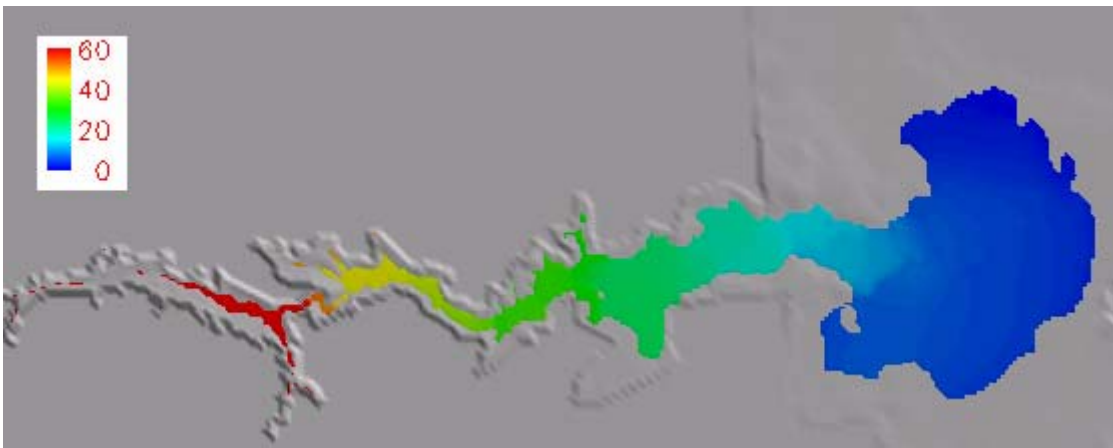
In the numerical simulations, two different meshes composed of 550×220 cells ($\Delta x = \Delta y = 30\text{m}$) and 1100×440 cells ($\Delta x = \Delta y = 15\text{m}$) respectively, were used. The initial water level in the reservoir was set to be 100 m above sea level. The rest of the computational domain was considered as dry bed. The initial discharge in the Reyran river, estimated to be in the range from 20 to 40 m^3/s , is neglected because it is much smaller than the flood discharge caused by the dam-break event, which is estimated to be the order of magnitude of 45,000 m^3/s (Valiani et al. 2002). The topographic data used in the simulation is obtained by interpolation based on the 13541 points of terrain elevation data on a triangulated irregular grid, which was used in the CADAM project. The Manning's coefficient was set to be $0.033 \text{ m}^{-1/3}$ over the entire computational domain, as suggested in the CADAM project (e.g. Goutal 1999 and Valiani et al. 2002). A total and instantaneous dam failure is considered. The time interval $\Delta t = 0.5 \text{ s}$ for the mesh with $\Delta x = \Delta y = 30\text{m}$, and $\Delta t = 0.25 \text{ s}$ for $\Delta x = \Delta y = 15\text{m}$ is used respectively in the simulation.

The computed water surface elevation at $t = 1200 \text{ s}$ and 2400 s after dam failure is presented in Figure 5. It shows that the numerical model gives a realistic prediction of the dam-break flow, including flooding in the downstream area as well as water receding in the reservoir area. It should be noted that above results are calculated with a mesh composed of 550×220 cells, that is $\Delta x = \Delta y = 30\text{m}$; no significant difference is found between the results from the coarse mesh ($\Delta x = \Delta y = 30\text{m}$) and the fine mesh ($\Delta x = \Delta y = 15\text{m}$).

In Figures 6 and 7, the computed maximum water level and wave front arrival time are compared with the measured data from physical model. It is shown that CCHE2D-FLOOD model reproduces major hydrodynamic behaviors of the flood event with reasonable accuracy. These figures also reveal that there is no significant difference between the results from the coarse mesh ($\Delta x = \Delta y = 30\text{m}$) and the fine mesh ($\Delta x = \Delta y = 15\text{m}$), except for the region near the dam site where the use of fine mesh yields better results, as shown at measurement points 6 and 7 in Figure 6. These figures show that the results from CCHE2D-FLOOD model are very close to the results from the model using approximate Riemann solvers with MUSCL approach (Valiani et al. 2002). However, their calculation with a final time $t=2800\text{s}$ and 10696 cells requires 26 hours on a PC with a Pentium III 700 MHz CPU, while the calculation by CCHE2D-FLOOD model with the same final time and 550×220 cells requires only 11 minutes on a PC with a Pentium III 850 MHz CPU. These results show that the CCHE2D-FLOOD model is accurate, robust and computationally efficient.



$t = 1200$ s



$t = 2400$ s

Figure 5. Water surface elevation (in meters)

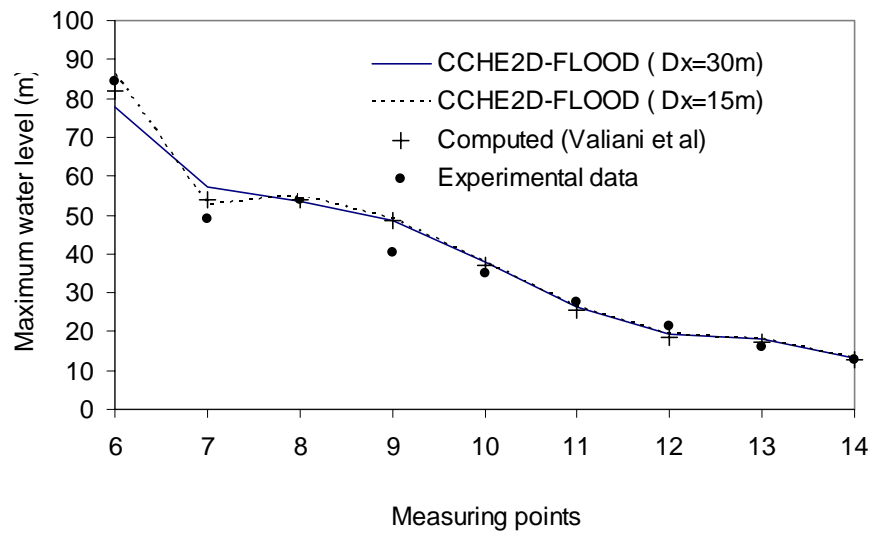


Figure 6. Comparison of computed maximum water level with measured data from physical model

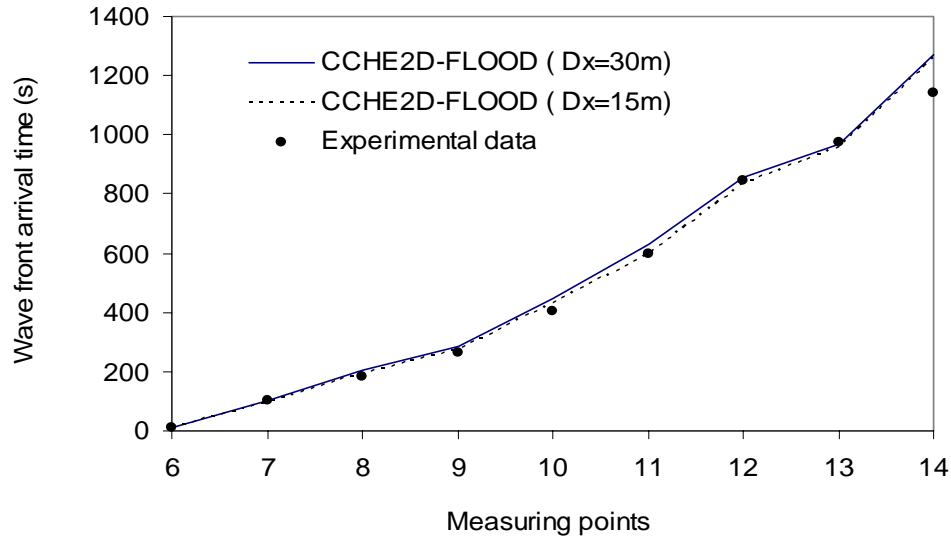


Figure 7. Comparison of computed wave front arrival time with measured data from physical model

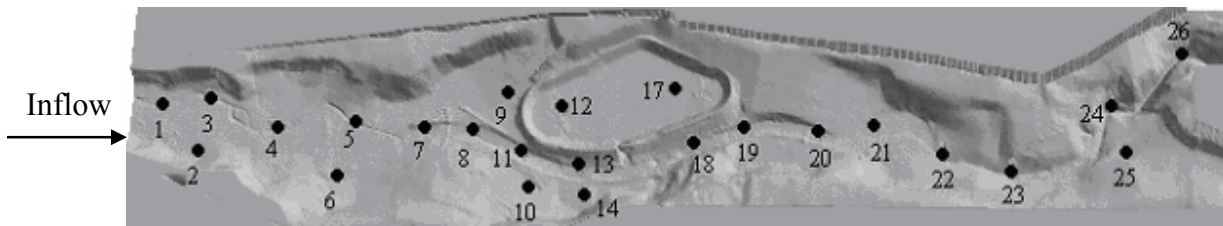


Figure 8. Topography of the Toce Valley and locations of stage gauges

3.3 Dam-break flow in the Toce valley

The numerical model is further validated against the experimental data measured in the physical model of a 5 km reach of the Toce valley located in the Northern Alps of Italy. The scale of the physical model is 1:100. The topography and locations of stage gauges are shown in Figure 8. Inflow discharge hydrograph is given in Fig.9. The valley is initially dry. This is a benchmark test case used in the CADAM project. The detailed description about this test case is presented in

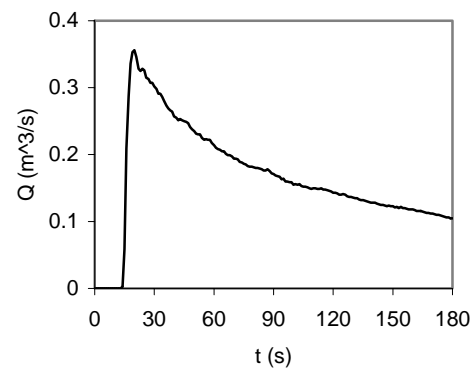


Figure 9. Inflow discharge hydrograph

the reference (Soares Frazao and Testa 1999). In the computation, the topographic data and the inflow discharge hydrograph of the physical model are employed so that the numerical results can be directly compared with the experimental data. The computational domain is discretized into square cells with $\Delta x = 0.05$ m, $\Delta y = 0.05$ m. The Manning coefficient is $0.0162 \text{ s/m}^{1/3}$, which is suggested by the CADAM project. The outflow boundary in the right end is set to be an open boundary. Figure 10 shows the computed results of dam-break flow in the Toce valley at different time. At $t=35$ s, flood wave reaches the embankment of the reservoir. The water surface outside the embankment

(around gauge No.9) ascends due to the influence of the embankment and overtopping flow occurs. Subsequently, more and more water flows into the reservoir, while flood wave continues to propagate along the valley. At $t=56.5$ s, flood wave reaches the location of gauge No. 26. It is estimated that the computed travel time from gauge No. 1 to No. 26 is 41 s, which is very close to the experimental data of 40 s and more accurate than the CADAM project participants' predictions of 50~58 s, as reported in the reference (Soares Frazao and Testa 1999). Figure 10 also shows that the water surface changes due to the deflection and reflection of irregular boundaries are well reproduced by the numerical model.

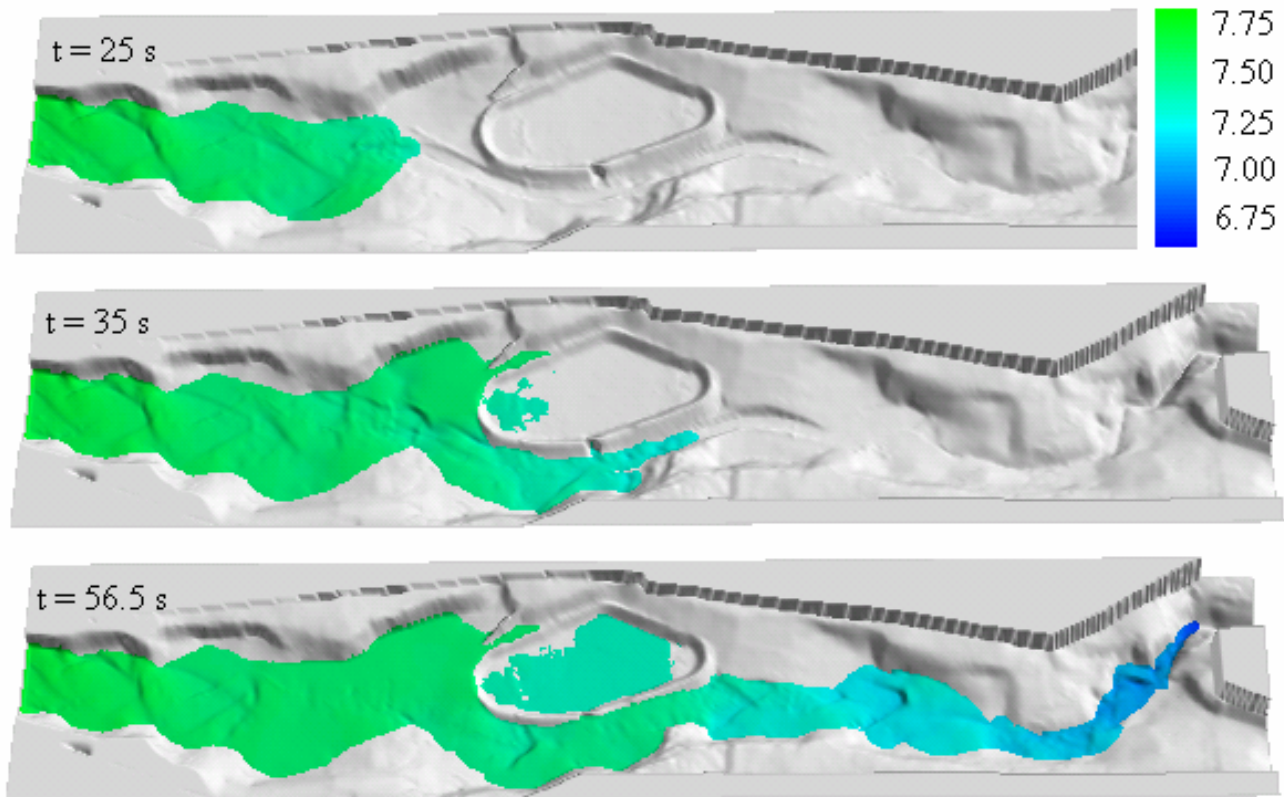
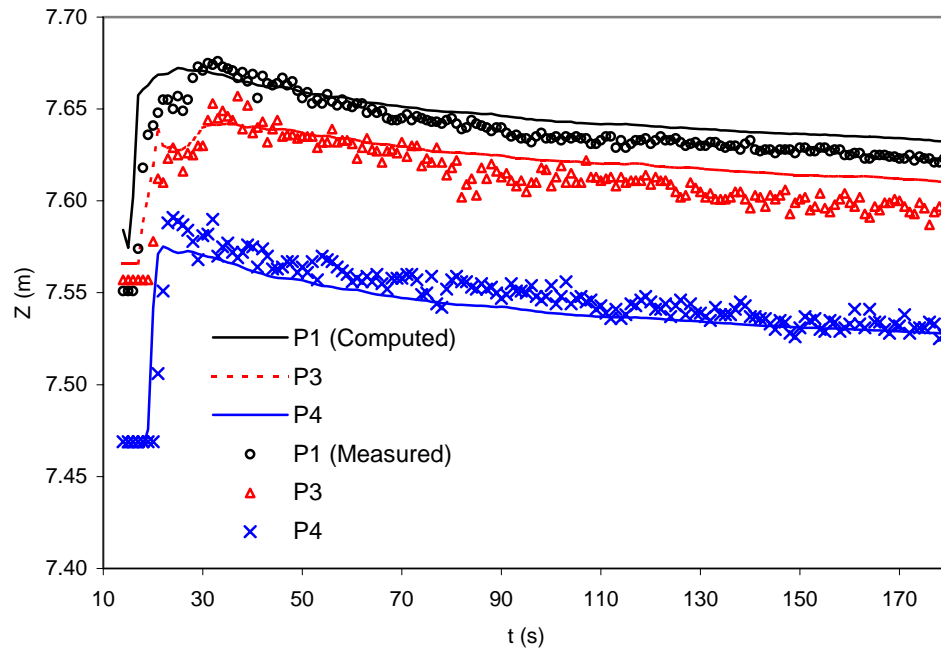
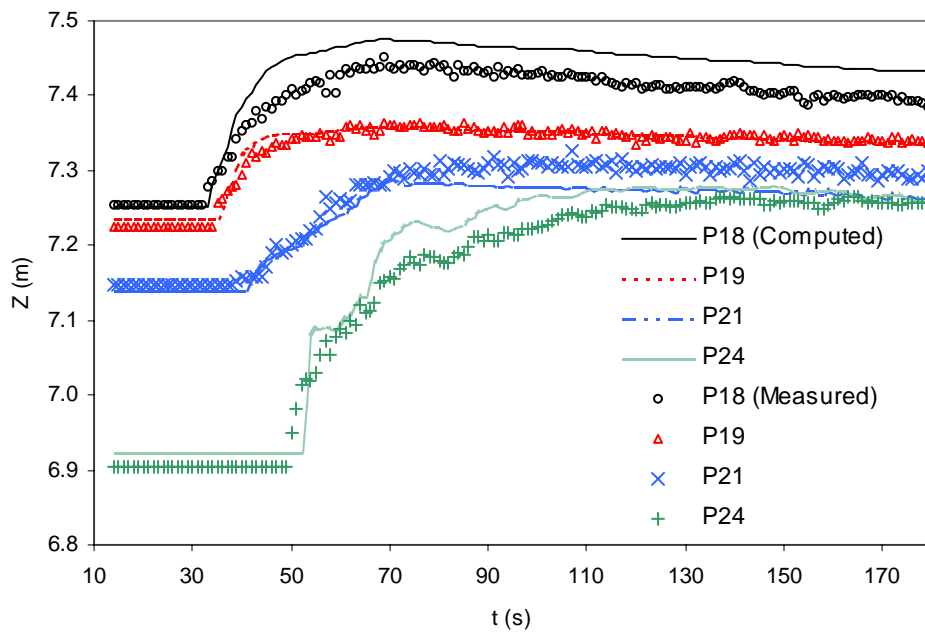


Figure 10. Computed results of dam-break flow in the Toce valley

Figure 11 further compares the numerical results and the experimental data at 7 measurement points. The overall agreement between them is satisfactory. It is not surprising that there is some discrepancy between the numerical results and the experimental data at individual points because buildings and two bridges in the valley are not taken into consideration in the computation. They may have influences on the local flow behavior.



(a) Upstream gauge points



(b) Downstream gauge points

Figure 11. Comparisons between numerical results and experimental results

CONCLUSIONS

The CCHE2D-FLOOD model is tested and validated using a partial dam-break test case and two real-life dam-break cases with complex topography. It is demonstrated that the model is capable to predict real life flood wave propagations due to dam and levee breach, which may includes supercritical flows, subcritical flows, transcritical flows, overtopping flows, as well as flooding and drying process. It is also found that the model performs well even in the case of complex topography.

ACKNOWLEDGMENTS

This work is a result of research sponsored by the USDA Agriculture Research Service under Specific Research Agreement No. 58-6408-2-0062 (monitored by the USDA-ARS National Sedimentation Laboratory) and by the US State Department Agency for International Development under Agreement No. EE-G-00-02-00015-00 and The University of Mississippi. The authors wish to thank Dr. Sandra Soares Frazao (University Catholique de Louvain) for providing valuable data set of the Malpasset dam-break case.

REFERENCES

- Goutal, N. (1999) "The Malpasset Dam Failure – An Overview and Test Case Definition", The Proceeding of the 4th CADAM meeting, Nov. 18-19, Zaragoza, Spain.
- Fracarollo, L. and Toro E. F. (1995). "Experimental and numerical assessment of the shallow water model for two-dimensional dam-break type problems." *J. of Hydraulic Research*, Vol.33, No.6, 843-864
- Soares Frazao, S. and Testa G. (1999). The Toce River test case: Numerical results analysis, *Proceedings of the 3rd CADAM workshop*, Milan
- Tseng, M. H. and Chu, C. R. (2000). "Two-dimensional shallow water flows simulation using TVD-MacCormac scheme." *J. of Hydraulic Research*, Vol.38, No.2, 123-131
- Valiani, A., Caleffi, V. and Zanni, A. (2002) "Case Study: Malpasset Dam-Break Simulation Using a Two-Dimensional Finite Volume Method" *J. Hydraulic Engineering*, ASCE, 128(5), 460-472
- Ying, X., Wang, S.S.Y. and Khan, A.A. (2003) "Numerical Simulation of Flood Inundation Due to Dam and Levee Breach", Proceeding of ASCE World Water & Environmental Resources Congress 2003 (CDROM), Philadelphia, USA, June 2003.
- Ying, X., Khan, A. and Wang, S.S.Y. (2004) "Upwind conservative scheme for the Saint Venant equation", *J. Hydraulic Engineering*, 130 (10), 977-987